

# Few-magnon physics in the spin- $S$ periodic $XXZ$ chain

Ning Wu,<sup>1,\*</sup> Hosho Katsura,<sup>2,3,4,†</sup> Sheng-Wen Li,<sup>1</sup> Xiaoming Cai,<sup>5</sup> and Xi-Wen Guan<sup>5,6,7,‡</sup>

<sup>1</sup>Center for Quantum Technology Research, School of Physics, Beijing Institute of Technology, Beijing 100081, China and Key Laboratory of Advanced Optoelectronic Quantum Architecture and Measurements (MOE), School of Physics, Beijing Institute of Technology, Beijing 100081, China

<sup>2</sup>Department of Physics, The University of Tokyo, 7-3-1 Hongo, Bunkyo-ku, Tokyo 113-0033, Japan

<sup>3</sup>Institute for Physics of Intelligence, The University of Tokyo, 7-3-1 Hongo, Bunkyo-ku, Tokyo 113-0033, Japan

<sup>4</sup>Trans-Scale Quantum Science Institute, University of Tokyo, Bunkyo-ku, Tokyo 113-0033, Japan

<sup>5</sup>State Key Laboratory of Magnetic Resonance and Atomic and Molecular Physics, Wuhan Institute of Physics and Mathematics, APM, Chinese Academy of Sciences, Wuhan 430071, China

<sup>6</sup>Center for Cold Atom Physics, Chinese Academy of Sciences, Wuhan 430071, China

<sup>7</sup>Department of Theoretical Physics, Research School of Physics and Engineering, Australian National University, Canberra ACT 0200, Australia

Few-magnon excitations in Heisenberg-like models play an important role in understanding magnetism and have long been studied by various approaches. However, the quantum dynamics of magnon excitations in a finite-size spin- $S$   $XXZ$  chain with single-ion anisotropy remains unsolved. Here, we exactly solve the two-magnon (three-magnon) problem in the spin- $S$   $XXZ$  chain by reducing the few magnons to a fictitious single particle on a one-dimensional (two-dimensional) effective lattice. Such a mapping allows us to obtain both static and dynamical properties of the model explicitly. The zero-energy states and various types of multimagnon bound states are manifested, with the latter being interpreted as edge states on the effective lattices. Moreover, we study the real-time multimagnon dynamics by simulating single-particle quantum walks on the effective lattices.

*Introduction.*—The Heisenberg  $XXZ$  model is a paradigmatic model exhibiting strong correlations. On the one hand, dynamical properties of the spin-1/2  $XXZ$  chain continue to attract the attention of the solid-state-physics community [1–4]. On the other hand, recent experimental advances in cold atom systems enable realizations of the  $XXZ$  chain and preparation of certain initial states [5, 6], even with higher spins [7], providing an ideal setting for studying nonequilibrium quantum dynamics. Recently, few-magnon dynamics in the spin-1/2  $XXZ$  chain has also attracted great theoretical interest [8, 9].

As an important theoretical problem, the few-magnon physics in Heisenberg-like models has long been studied by a variety of theoretical approaches [10–25]. Among these, the center-of-mass method provides a physically intuitive way to view the few-magnon problem as a single-particle one [22, 25]. In spite of these developments, to the best of our knowledge, a mathematically rigorous treatment of the three-magnon problem for a finite-size higher-spin  $XXZ$  chain is still missing. In this Letter, we construct exact Bloch states that achieve block diagonalization of the two- and three-magnon sectors in a finite-size spin- $S$   $XXZ$  chain with single-ion anisotropy. This converts the two-magnon (three-magnon) problem into a single-particle one on a one-dimensional (two-dimensional) effective lattice whose size scales linearly

(quadratically) with the total number of sites. Our method thus provides an exact, intuitive, and convenient way to understand the few-magnon physics.

We employ our formalism to study several aspects of the model. We first discover the condition under which the few-magnon excitation energy with respect to the ferromagnetic state exactly vanishes and obtain explicit forms of these zero-energy states (ZESs). In certain parameter regimes, we reveal various types of three-magnon bound states, which turn out to be localized edge states on the effective lattice. We then calculate the three-magnon dynamics from localized spin states via simulating single-particle quantum walks on the forgoing lattice. Several perturbative approaches are employed to interpret the observed dynamical behavior of the magnetization diffusion, demonstrating the essential role played by the multimagnon bound states in the dynamics.

*Model and methodology.*—The spin- $S$   $XXZ$  chain with  $N$  spins is described by the Hamiltonian

$$\begin{aligned}
 H &= -J_{xy}H_{XY} - J_zH_Z - DH_D, \\
 H_{XY} &= \sum_{j=1}^N (S_j^x S_{j+1}^x + S_j^y S_{j+1}^y), \\
 H_Z &= \sum_{j=1}^N S_j^z S_{j+1}^z, \quad H_D = \sum_{j=1}^N (S_j^z)^2, \quad (1)
 \end{aligned}$$

where  $\vec{S}_j = (S_j^x, S_j^y, S_j^z)$  is the spin operator on site  $j$  with quantum number  $S \geq 1/2$ ,  $J_{xy}$  and  $J_z$  are the exchange interactions between nearest-neighboring spins, and  $D \geq 0$  is the single-ion anisotropy strength. We assume that

\*Electronic address: wunwyz@gmail.com

†Electronic address: katsura@phys.s.u-tokyo.ac.jp

‡Electronic address: xwe105@wipm.ac.cn

$N$  is even and impose periodic boundary conditions. We focus on the case of  $J_z > 0$  and take the ferromagnetic state  $|F\rangle = |S, S, \dots, S\rangle$  as a reference state possessing eigenenergy  $E_F = -NS^2(J_z + D)$ , though our formalism is valid for both ferromagnetic and antiferromagnetic chains near saturation magnetization [1]. The single-magnon states are simply  $|\psi(k)\rangle = \frac{1}{\sqrt{N}} \sum_{n=0}^{N-1} e^{ikn} T^n |1\rangle$  with  $T$  the translation operator satisfying  $T|j\rangle = |j+1\rangle$  (here, the normalized state  $|j_1 \dots j_n\rangle \equiv C S_{j_1}^- \dots S_{j_n}^- |F\rangle$  with suitable normalization coefficient  $C$ ). We choose  $k \in K_0 = \{\frac{2\pi l}{N} | l = -\frac{N}{2}, -\frac{N}{2} + 1, \dots, \frac{N}{2} - 1\}$  to ensure the translational invariance of  $|\psi(k)\rangle$ . It has an excitation energy  $\mathcal{E}(k) \equiv E(k) - E_F = 2S(J_z - J_{xy} \cos k) + D(2S - 1)$  with  $H|\psi(k)\rangle = E(k)|\psi(k)\rangle$ .

Below we mainly focus on the more subtle three-magnon sector and one can refer to Ref. [26] for a detailed construction of the two-magnon Bloch states. We assume  $S \geq 3/2$  and  $N = 3m$  (hence  $m = \text{even}$ ) for simplicity. There are three types of real-space basis states: i)  $|j_1, j_1, j_1\rangle$  ( $1 \leq j_1 \leq N$ ), ii)  $|j_1, j_1, j_2\rangle$  and  $|j_1, j_2, j_2\rangle$  ( $1 \leq j_1 < j_2 \leq N$ ), and iii)  $|j_1, j_2, j_3\rangle$  ( $1 \leq j_1 < j_2 < j_3 \leq N$ ), forming a complete basis of the  $\mathcal{D} = N(N+1)(N+2)/6$ -dimensional three-magnon sector. We now define two sets of wave numbers,  $K_2 = \{\frac{2\pi l}{m} | l = -\frac{m}{2}, -\frac{m}{2} + 1, \dots, \frac{m}{2} - 1\}$  and  $K'_2 = K_0 \setminus K_2$ . An element  $k$  from  $K_2$  ( $K'_2$ ) satisfies  $e^{ikm} = 1$  ( $e^{ikm} \neq 1$ ). For any  $k \in K'_2$ , we construct the  $\bar{\mathcal{D}} = (N^2 + 3N)/6$  Bloch states

$$|\psi_{r_1, r_2}(k)\rangle = e^{r_1 i \frac{k}{3}} e^{(r_1 + r_2) i \frac{k}{3}} \frac{1}{\sqrt{N}} \sum_{n=0}^{N-1} e^{ikn} |\phi_{r_1, r_2}^n\rangle, \quad (2)$$

where  $r_1 = 0, 1, \dots, m-1$  and  $r_1 \leq r_2 \leq N - (2r_1 + 1)$ , and  $|\phi_{r_1, r_2}^n\rangle \equiv T^n |1, 1+r_1, 1+r_1+r_2\rangle$  is a typical localized state. For any  $k \in K_2$ , we similarly construct the  $\bar{\mathcal{D}}$  states  $\{|\psi_{r_1, r_2}(k)\rangle\}$ , as well as an additional Bloch state

$$|\psi_{m, m}(k)\rangle = \frac{e^{ikm}}{\sqrt{m}} \sum_{n=0}^{m-1} e^{ikn} |\phi_{m, m}^n\rangle. \quad (3)$$

These define a complete set of  $2m\bar{\mathcal{D}} + m(\bar{\mathcal{D}} + 1) = \mathcal{D}$  Bloch states that achieve an exact block diagonalization of the three-magnon sector in a finite-size chain.

The  $\bar{\mathcal{D}} + 1$  states  $\{|\psi_{r_1, r_2}(k \in K_2)\rangle\}$  define a single-particle problem described by  $\mathcal{H}_3(k)$  on a triangle-shape two-dimensional lattice in the  $r_1$ - $r_2$  plane. Straightforward analysis results in a graphical representation of off-diagonal part,  $H_{XY}$ , as shown in Fig. 1 [for  $k \in K'_2$  we simply remove the site  $(r_1, r_2) = (m, m)$ ]. The complex hoppings between the Bloch states are represented by lines with arrows between different sites. It is worth mentioning that similar ideas have been developed in Refs. [22] and [25] for infinite chains. However, to the best of our knowledge, the exact Bloch states given by Eqs. (2) and (3) provide the first mathematically rigorous construction for the Bloch basis in the three-magnon sector for a finite-size higher-spin  $XXZ$  chain.

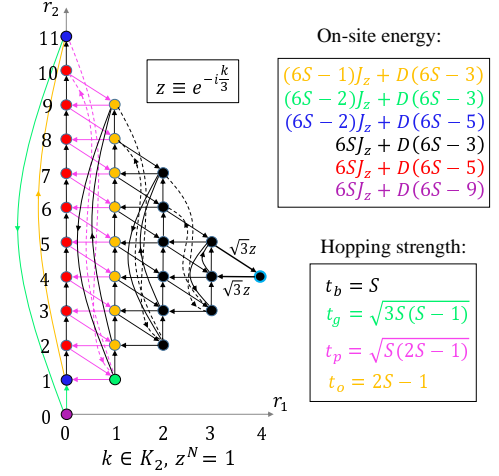


FIG. 1: Representations of  $H_{XY}$  on an effective two-dimensional lattice formed by the Bloch basis states  $\{|\psi_{r_1, r_2}(k)\rangle\}$  for  $k \in K_2$  ( $N = 12$  as an example). Nonvanishing complex hopping between two Bloch states is represented by an arrowed line, with the color and arrow indicating its magnitude and the corresponding phase factor  $z = e^{-i\frac{k}{3}}$ , respectively. The colors of the circles indicate different eigenenergies of  $\mathcal{H}_3(k)|_{J_{xy}=0} - E_F$ . The effective lattice for  $k \in K'_2$  is obtained by removing the rightmost circle ( $m, m$ ).

$D = 0$ : zero-energy states.-In the case of  $D = 0$  and for a fixed  $k \in K_0$ , it is easy to see that the single-magnon excitation energy  $\mathcal{E}(k)$  vanishes when the following condition is satisfied,

$$J_z = J_{xy} \cos k, \quad k \in K_0. \quad (4)$$

The corresponding (unnormalized) single-magnon state is given by  $L_k|F\rangle$ , where  $L_k \equiv \sum_{j=1}^N e^{ikj} S_j^-$ . In Ref. [26] we show that  $(L_k)^n|F\rangle$  is indeed a zero-energy state in the  $n$ -magnon sector once (4) is fulfilled, i.e.,  $(H - E_F)(L_k)^n|F\rangle = 0$  with  $n \leq 2NS + 1$ . These ZESs are interesting since linear combinations of them are relevant to the so-called spin helix state [27], which has recently been experimentally prepared for  $S = 1/2$  [6].

As an eigenstate of  $H$ ,  $(L_k)^n|F\rangle$  must also be a zero-energy eigenstate of a certain Bloch Hamiltonian  $\mathcal{H}_n(p) - E_F$ , with  $p = p(k)$  a function of  $k$  to be determined. For  $n = 1$ , it is obvious that  $p(k) = k$ . For  $n = 2$ , we analytically show that the ZES  $(L_k)^2|F\rangle$  is consistent with the zero-energy Bloch state, which is also the ground state, of  $\mathcal{H}_2(p) - E_F$ , where  $p(k)$  is given by [26]

$$p(k) = \begin{cases} 2k, & k \in [-\frac{\pi}{2}, 0], \\ 2k + 2\pi, & k \in [-\pi, -\frac{\pi}{2}). \end{cases} \quad (5)$$

For  $n = 3$ , we find that [see Fig. 2(a)]

$$p(k) = \begin{cases} 3k, & k \in [-\frac{\pi}{3}, 0], \\ 3k + 2\pi, & k \in [-\pi, -\frac{\pi}{3}). \end{cases} \quad (6)$$

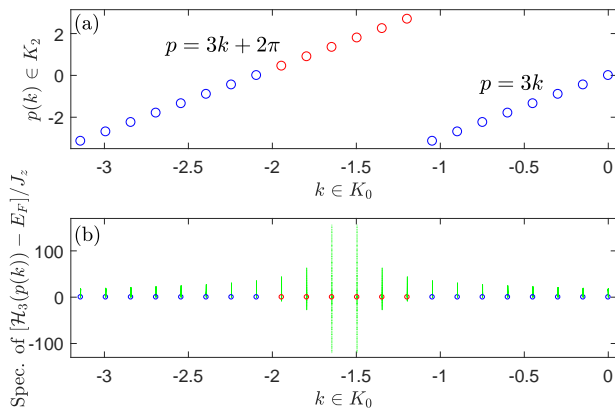


FIG. 2: The ZES  $(L_k)^3|F\rangle$  is equivalent to the zero-energy eigenstate of  $\mathcal{H}_3(p(k)) - E_F$  under the condition  $J_z = J_{xy} \cos k$ , where  $p(k)$  is given by Eq. (6). (a)  $p(k) \in K_2$  as a function of  $k \in K_0$ . (b) The full spectrum (green points) of  $\mathcal{H}_3(p(k)) - E_F$ . A blue (red) circle indicates that the corresponding ZES  $(L_k)^3|F\rangle$  is the ground state (an excited state) of  $\mathcal{H}_3(p(k)) - E_F$ . Parameters:  $N = 42$ ,  $S = 2$ .

which actually belongs to  $K_2$ . Figure 2(b) shows the full spectrum (green points) of  $\mathcal{H}_3(p(k)) - E_F$  under the condition (4) for each  $k \in K_0$ . Except for the middle region  $k \in (-\frac{2}{3}\pi, -\frac{\pi}{3})$  (red circles), the ZES  $(L_k)^3|F\rangle$  is also found to be the ground state (blue circles) of the corresponding Bloch Hamiltonian  $\mathcal{H}_3(p) - E_F$ . We believe some of these properties persist in sectors with higher numbers of magnons. For example, in the  $n$ -magnon sector (suppose  $N$  is divisible by  $n$ ) the ZES  $(L_k)^n|F\rangle$  with  $k \in [-\frac{\pi}{n}, 0]$  should be the ground state of  $\mathcal{H}_n(nk) - E_F$ .

*Multimagnon bound states and dynamics.*— The Bloch Hamiltonian  $\mathcal{H}_3(k)$  is diagonal in the case of  $J_{xy} = 0$ . From Fig. 1 we see that the ground state of  $\mathcal{H}_3(k)|_{J_{xy}=0}$  for  $D/J_z > 1/2$  ( $D/J_z < 1/2$ ) is  $|\psi_{0,0}(k)\rangle$  (are  $|\psi_{0,1}(k)\rangle$  and  $|\psi_{0,N-1}(k)\rangle$ ), which will be referred to as the  $p$ -state (purple) [ $b$ -states (blue)] according to the colors of the solid circles. Turning on the  $xy$ -interaction generally mixes these states to form quasi-continuous bands. However, bound states separated from the continua can emerge in certain parameter regimes.

Figure 3(a)-(f) show the three-magnon excitation spectra calculated by numerically diagonalizing the Bloch Hamiltonians  $\{\mathcal{H}_3(k)\}$  for  $N = 42$  and  $S = 2$ . We observe several separate branches that indicate the emergence of bound states. For  $D = 0$  and  $J_{xy} = 0$ , the two  $b$ -states are degenerate with the  $g$ -state (green,  $|\psi_{1,1}(k)\rangle$ ). We use Takahashi's many-body perturbation theory [28] to derive an effective Hamiltonian  $\mathcal{H}_{3,D=0}^{(\text{eff})}(k) - E_F$  (up to third order of  $J_{xy}/J_z$ , see [26]) in this three-dimensional degenerate manifold. The dashed curves in Fig. 3(a) represent the three eigenenergies of  $\mathcal{H}_{3,D=0}^{(\text{eff})}(k) - E_F$  for  $J_{xy}/J_z = 0.1$ , which are in good agreement with the exact results. As  $D/J_z$  increases to 0.4 [Fig. 3(b)], the  $p$ -,  $g$ -, and  $b$ -states are responsible for the four separated

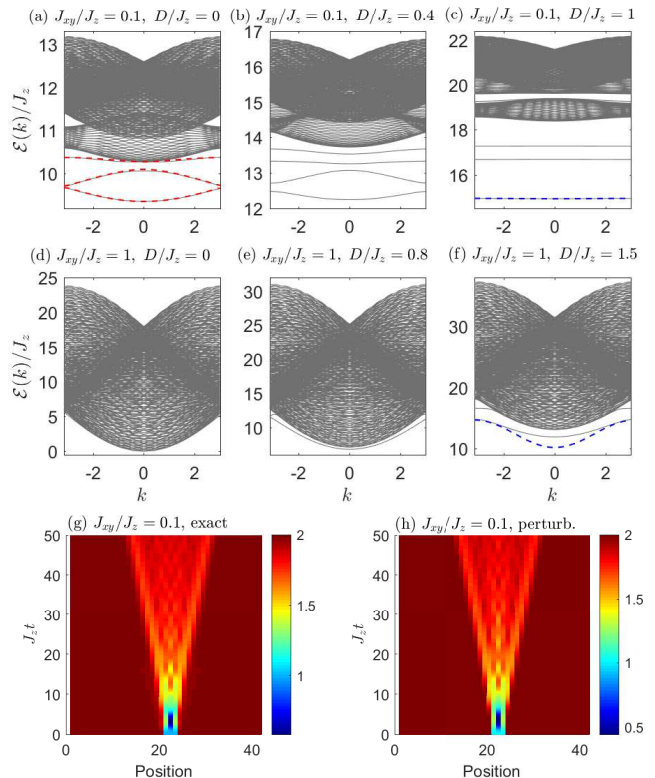


FIG. 3: (a)-(f) Three-magnon excitation spectra for  $N = 42$ ,  $S = 2$ . The dashed curves in (a), (c), and (f) show the perturbative results. (g) Magnetization dynamics  $\langle S_j^z(t) \rangle$  from an initial state  $|\frac{N}{2}, \frac{N}{2}+1, \frac{N}{2}+2\rangle$  for  $J_{xy}/J_z = 0.1$ . (h) The corresponding approximated dynamics using the effective Hamiltonian  $\mathcal{H}_{3,D=0}^{(\text{eff})}(k)$ .

levels. In the large anisotropy limit with  $D/J_z = 1$  [Fig. 3(c)], the lowest branch of the spectrum is dominated by the nondegenerate  $p$ -state. A fourth-order nondegenerate perturbative calculation of the lowest eigenenergy [26] agrees well with the exact result [dashed curve in Fig. 3(c)]. The middle quasi-continuous band around  $\mathcal{E}(k)/J_z = 19$  is due to the mixing of the  $N - 3$  edge  $r$ -states (red) and the  $g$ -state.

The middle panels of Fig. 3 show the spectrum for  $J_{xy}/J_z = 1$ . Compared with the case of small  $J_{xy}/J_z$ , a larger  $D$  is needed to observe the bound states. Nevertheless, the lowest branches in Fig. 3(e) and (f) are still dominated by the  $p$ -states. The fourth-order perturbation still gives accurate results for the spectrum at the edges of the momentum space [dashed curve in Fig. 3(f)].

The foregoing identification of magnon bound states provides an intuitive way to look at the multimagnon dynamics. Suppose the system is initially prepared in a localized state  $|\Phi(0)\rangle = |\phi_{r_1, r_2}^n\rangle$ . We are interested in the local magnetization dynamics  $\langle S_j^z(t) \rangle =$

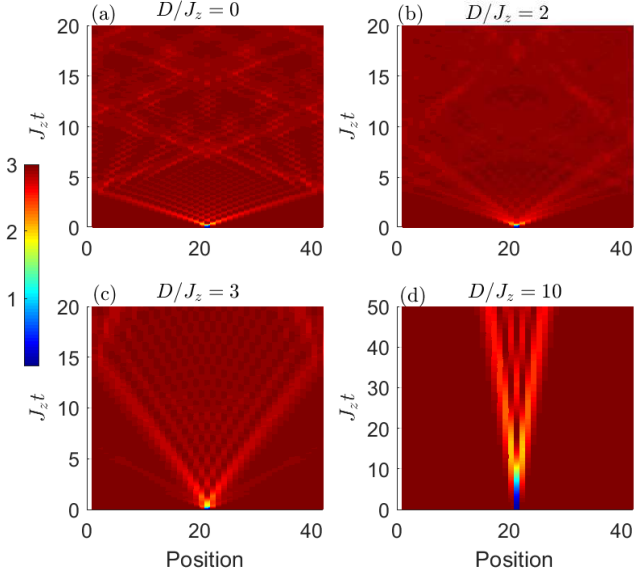


FIG. 4: Magnetization dynamics  $\langle S_j^z(t) \rangle$  from an initial state  $|\frac{N}{2}, \frac{N}{2}, \frac{N}{2}\rangle$  for  $J_{xy}/J_z = 1$ ,  $N = 42$ , and  $S = 3$ . (a)  $D/J_z = 0$ , (b)  $D/J_z = 2$ , (c)  $D/J_z = 3$ , (d)  $D/J_z = 10$ .

$\langle \Phi(0) | e^{iHt} S_j^z e^{-iHt} | \Phi(0) \rangle$ , which can be expressed as [26]:

$$\langle S_j^z(t) \rangle = S - \sum_{a=1}^3 \sum_{s_1 s_2=(0,0)}^{(m-1, m+1)} |X_{r_1 r_2; s_1 s_2}^{(a), j, n}(t)|^2 - |Y_{r_1 r_2}^{j, n}(t)|^2. \quad (7)$$

Explicit expressions for the  $X$ 's and  $Y$  can be found in [26]. It turns out that these quantities are mainly contributed by eigenstates having significant overlap with the initial component state  $|\psi_{r_1, r_2}(k)\rangle$  [29].

Figure 3(g) shows the evolution of  $\langle S_j^z(t) \rangle$  starting with  $|\Phi(0)\rangle = |\phi_{1,1}^{\frac{N}{2}-1}\rangle = |\frac{N}{2}, \frac{N}{2} + 1, \frac{N}{2} + 2\rangle$  for  $D = 0$  and  $J_{xy}/J_z = 0.1$ . The situation here is quite similar to a three-boson quantum walk recently studied in Ref. [30]. We expect that the three-magnon bound states shown in Fig. 3(a) can accurately capture the magnetization dynamics since  $|\phi_{1,1}^{\frac{N}{2}-1}\rangle$  is a linear combination of the  $g$ -states. To this end, we use the  $3 \times 3$  effective Hamiltonian  $\mathcal{H}_{3, D=0}^{(\text{eff})}(k)$  [26] to calculate  $\langle S_j^z(t) \rangle$  [Fig. 3(h)], which is found to agree well with the result obtained by full quantum simulation. However, deviation from the exact dynamics is observed for a larger hopping with  $J_{xy}/J_z > 0.1$ , due to the fact that the highest effective level starts merging into the upper continuous band (data not shown).

Figure 4 shows  $\langle S_j^z(t) \rangle$  starting with  $|\phi_{0,0}^{\frac{N}{2}-1}\rangle = |\frac{N}{2}, \frac{N}{2}, \frac{N}{2}\rangle$  for  $J_{xy}/J_z = 1$ ,  $S = 3$  and several values of  $D/J_z$ . The propagation of the profile narrows down as  $D/J_z$  increases. To understand the short-time dynamics in the small and large  $D$  limits, we perform a second

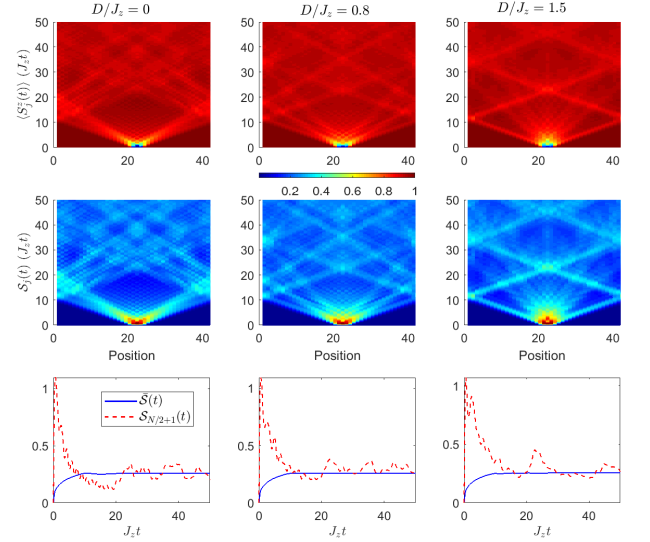


FIG. 5: Time evolution of  $\langle S_j^z(t) \rangle$  (top row),  $\mathcal{S}_j(t)$  (middle row), and  $\bar{S}(t)$  and  $\mathcal{S}_{N/2+1}$  (bottom row) for an initial state  $|\frac{N}{2}, \frac{N}{2} + 1, \frac{N}{2} + 2\rangle$  and  $J_{xy}/J_z = 1$ ,  $N = 42$ , and  $S = 1$ .

order time-dependent analysis, leading to [26]

$$\langle S_j^z(t) \rangle \approx S - 3\delta_{j, \frac{N}{2}} + 6J_{xy}^2 S(S-1) \frac{1 - \cos \varepsilon_{pb} t}{\varepsilon_{pb}^2} (2\delta_{j, \frac{N}{2}} - \delta_{j, \frac{N}{2}+1} - \delta_{j, \frac{N}{2}-1}), \quad (8)$$

where  $\varepsilon_{pb} \equiv 2(J_z - 2D)$  is the energy difference between the  $p$ - and  $b$ -states. The spin flips therefore mainly spread to nearest neighbors at short times and the corresponding local magnetizations oscillate with a period of  $2\pi/\varepsilon_{pb}$ .

*Growth of total correlation for  $S = 1$ .*—Recently, a spin-1 ferromagnetic  $XXX$  model with single-ion anisotropy has been realized with ultracold atoms [7]. For  $S = 1$ , it can be shown that the reduced density matrix  $\rho_j(t)$  for site  $j$  is diagonal and solely determined by  $\langle S_j^z \rangle$  and  $\langle (S_j^z)^2 \rangle$  [26]:  $\rho_j(t) = \text{diag}[\langle (S_j^z)^2 \rangle + \langle S_j^z \rangle / 2, 1 - \langle (S_j^z)^2 \rangle, \langle (S_j^z)^2 \rangle - \langle S_j^z \rangle / 2]$ . We are interested in the entanglement between site  $j$  and the rest of the system measured by the von Neumann entropy  $\mathcal{S}_j(t) = -\text{Tr} \rho_j(t) \ln \rho_j(t)$ . We also consider the average entropy  $\bar{S}(t) \equiv \sum_j \mathcal{S}_j(t) / N$ , which is related to the total correlation entropy  $\mathcal{T}$  of the time evolved state  $\rho(t)$  via  $\mathcal{T} = N\bar{S}(t)$  [31–33]. The first two rows of Fig. 5 show the time evolution of  $\langle S_j^z(t) \rangle$  and  $\mathcal{S}_j(t)$  for an initial state  $|\frac{N}{2}, \frac{N}{2} + 1, \frac{N}{2} + 2\rangle$ . We see that  $\langle S_j^z(t) \rangle$  and  $\mathcal{S}_j(t)$  exhibit similar diffusive patterns. The bottom row of Fig. 5 shows the evolution of the averaged entropy  $\bar{S}(t)$  and the single-site entropy on site  $N/2 + 1$ . Although each single site shows complicated entropy dynamics, the total correlation approximately exhibits a monotonically increasing behavior and approaches a steady value  $\mathcal{T}/N \approx 0.26$  for  $N = 42$  we considered. This is relevant to the irreversible entropy increase in thermodynamics [34, 35].

To understand the long-time behavior of  $\mathcal{T}/N$ , we assume that at long times the single-site state of an arbitrary spin is approximated by a diagonal density matrix  $\sigma = \text{diag}(P_1, P_0, P_{-1})$  (in the basis  $\{|1\rangle, |0\rangle, |-1\rangle\}$ ). We intend to maximize the quantities  $\mathcal{S}^{(\sigma)}(t) = -\sum_{n=0,\pm 1} P_n \ln P_n$  in the state  $\sigma$  under the constraints of probability normalization  $\sum_{n=0,\pm 1} P_n = 1$  and magnetization conservation  $\sum_{n=0,\pm 1} n P_n = (N-3)/N$  [34]. Standard Lagrangian multiplier analysis gives  $\max \mathcal{S}^{(\sigma)}(t) = 0.2621$  for  $N = 42$  [26]. The good agreement between the exact result and the above picture indicates that the total correlation of  $\rho(t)$  approaches the value given by a pseudo-equilibrium state  $\rho_{p\text{-eq}} \equiv \otimes_j \sigma_j$  in the long-time limit.

*Conclusions and Discussions*—In this work, we provide the first construction of exact Bloch states realizing the block diagonalization of the three-magnon sector in a finite-size higher-spin periodic  $XXZ$  chain. Each block Bloch Hamiltonian defines a single-particle problem on a two-dimensional triangle-shape lattice. Several types of magnon bound states are identified as edge states on the foregoing lattice. By diagonalizing the Bloch Hamilto-

nians in the absence of the single-ion anisotropy, we revealed the condition under which zero-excitation-energy states upon the ferromagnetic state emerge. As an application of our formalism, we studied the multimagnon dynamics by simulating single-particle quantum walks on the effective lattices. The spread of local excitations over the chain is explained in terms of magnon bound states in certain parameter regimes. We also studied the total correlation growth starting with a localized three-magnon state in a spin-1 Heisenberg chain which was recently realized in cold atoms. It is found that the long-time total correlation is well approximated by its value in a particular pseudo-equilibrium state.

**Acknowledgements:** This work was supported by the Natural Science Foundation of China (NSFC) under Grant No. 11705007, and partially by the Beijing Institute of Technology Research Fund Program for Young Scholars. H.K. was supported in part by JSPS Grant in-Aid for Scientific Research on Innovative Areas No. JP20H04630, JSPS KAKENHI Grant No. JP18K03445, and the Inamori Foundation. X.-W.G. was supported by the NSFC Grant No. 11874393.

- 
- [1] A. Keselman, L. Balents, and O. A. Starykh, Phys. Rev. Lett. **125**, 187201 (2020).
- [2] A. K. Bera, J. Wu, W. Yang, R. Bewley, M. Boehm, J. Xu, M. Bartkowiak, O. Prokhnenko, B. Klemke, A. T. M. N. Islam, J. M. Law, Z. Wang, and B. Lake, Nat. Phys. **16**, 625 (2020).
- [3] P. Chauhan, F. Mahmood, H. J. Changlani, S. M. Koochpayeh, and N. P. Armitage, Phys. Rev. Lett. **124**, 037203 (2020).
- [4] C. Babenko, F. Göhmann, K. K. Kozłowski, J. Sirker, and J. Suzuki, Phys. Rev. Lett. **126**, 210602 (2021).
- [5] T. Fukuhara, P. Schauß, M. Endres, S. Hild, M. Cheneau, I. Bloch, and C. Gross, Nature (London) **502**, 76 (2013).
- [6] P. N. Jepsen, J. Amato-Grill, I. Dimitrova, W. W. Ho, E. Demler, and W. Ketterle, Nature **588**, 403 (2020).
- [7] W. C. Chung, J. de Hond, J. Xiang, E. Cruz-Colón, and W. Ketterle, Phys. Rev. Lett. **126**, 163203 (2021).
- [8] M. Ganahl, E. Rabel, F. H. L. Essler, and H. G. Evertz, Phys. Rev. Lett. **108**, 077206 (2012).
- [9] W. Liu and N. Andrei, Phys. Rev. Lett. **112**, 257204 (2014).
- [10] M. Wortis, Phys. Rev. **132**, 85 (1963).
- [11] A. M. Bonnot and J. Hanus, Phys. Rev. B **7**, 2207 (1973).
- [12] A. A. Bahurmuz and P. D. Loly, J. Phys. C **19**, 2241 (1986).
- [13] R. Silbergliitt and J. B. Torrance, Jr., Phys. Rev. B **2**, 772 (1970).
- [14] T. Oguchi, J. Phys. Soc. Jpn. **31**, 394 (1971).
- [15] J. E. Van Himbergen and J. A. Tjon, Physica **76**, 503 (1974).
- [16] T. Schneider, Phys. Rev. B **24**, 5327 (1981).
- [17] N. Papanicolaou and G. C. Psaltakis, Phys. Rev. B **35**, 342 (1987).
- [18] P. N. Bibikov, J. Stat. Mech. (2016) 033109.
- [19] J. Hanus, Phys. Rev. Lett. **11**, 336 (1963).
- [20] S. C. Bell, P. D. Loly, and B. W. Southern, J. Phys.: Condens. Matter **1**, 9899 (1989).
- [21] B. W. Southern, T. S. Liu, D. A. Lavis, Phys. Rev. B **39**, 12160 (1989).
- [22] B. W. Southern, R. J. Lee, and D. A. Lavis, J. Phys.: Condens. Matter **6**, 10075 (1994).
- [23] S. L. M. Cyr, B. W. Southern, and D. A. Lavis, J. Phys.: Condens. Matter **8**, 4781 (1996).
- [24] B. W. Southern, J. L. M. Cuéllar, and D. A. Lavis, Phys. Rev. B **58**, 9156 (1998).
- [25] L. Kecke, T. Momoi, and A. Furusaki, Phys. Rev. B **76**, 060407(R) (2007).
- [26] See Supplemental Materials for details.
- [27] V. Popkov and G. M. Schütz, Phys. Rev. E **95**, 042128 (2017).
- [28] M. Takahashi, J. Phys. C **10**, 1289 (1977).
- [29] A local state  $|\phi_{r_1, r_2}^n\rangle$  can generally be expanded in terms of the Bloch states as  $|\phi_{r_1, r_2}^n\rangle = \frac{1}{\sqrt{N}} \sum_{k \in K_0} e^{-ikn} e^{-i\frac{k}{3}(2r_1+r_2)} |\psi_{r_1, r_2}(k)\rangle$  [for  $(r_1, r_2) \neq (m, m)$ ] or  $|\phi_{m, m}^n\rangle = \frac{1}{\sqrt{m}} \sum_{k \in K_2} e^{-ikm} e^{-ikn} |\psi_{m, m}(k)\rangle$ .
- [30] X. Cai, H. Yang, H.-L. Shi, C.-H. Li, N. Andrei, and X.-W. Guan, arXiv:2103.07843.
- [31] D. L. Zhou, Phys. Rev. Lett. **101**, 180505 (2008).
- [32] S. Watanabe, IBM J. Res. Dev. **4**, 66 (1960).
- [33] B. Groisman, S. Popescu, and A. Winter, Phys. Rev. A **72**, 032317 (2005).
- [34] S.-W. Li, C. P. Sun, Phys. Rev. A **103**, 042201 (2021).
- [35] F. Anza, F. Pietracaprina, and J. Goold, Quantum **4**, 250 (2020).
-



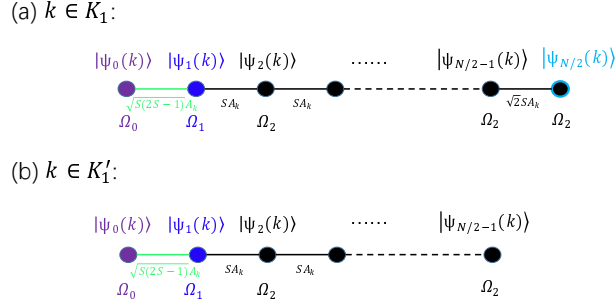


FIG. 6: The effective one-dimensional lattice formed by the Bloch states in the two-magnon sector with wave numbers drawn from (a)  $k \in K_1$  and (b)  $k \in K'_1$ .

Physically, we can view  $\mathcal{H}_2(k \in K_1)$  [ $\mathcal{H}_2(k \in K'_1)$ ] as a single-particle problem on an effective one-dimensional lattice with  $N/2 + 1$  ( $N/2$ ) sites, with the nearest-neighboring hopping proportional to  $A_k$  and the on-site energies being  $\Omega_i$  (see Fig. 6). Let us consider the case of  $N = 4l$  ( $l \in Z$ ), so that  $k = -\pi \in K_1$ , and hence  $\mathcal{H}_2(k = -\pi)$  is diagonal. The two eigenstates  $|\psi_0(-\pi)\rangle$  and  $|\psi_1(-\pi)\rangle$ , which are respectively referred to as the single-ion and exchanged two-magnon bound states in Ref. [1], were also revealed in the Bethe ansatz solution [2]. Note that  $\Omega_1 - \Omega_0 = 2D - J_z$ , so the single-ion bound state is dominated for  $D/J_z > 1/2$  [3]. It is interesting to note that the two types of bound states correspond to two localized edge states on the effective lattice. The remaining  $N/2 - 1$  state  $|\psi_r(-\pi)\rangle$  ( $r = 2, 3, \dots, N/2$ ) are degenerate and possess eigenenergy  $\Omega_2 \geq \Omega_0, \Omega_1$ . They correspond to two-magnon scattering states.

## Appendix B: The zero-energy states

### 1. Proof of $(H - E_F)(L_k)^n|F\rangle = 0$ under the condition $J_z = J_{xy} \cos k, k \in K_0$

For a given  $k \in K_0$ , we will show that the state  $(L_k)^n|F\rangle$  is an eigenstate of  $H - E_F$  with zero energy, i.e.,

$$(H - E_F)(L_k)^n|F\rangle = 0, \quad n = 1, 2, \dots, 2NS + 1, \quad (\text{B1})$$

provided the following condition is satisfied:

$$J_z = J_{xy} \cos k. \quad (\text{B2})$$

Note that for  $n > 2NS + 1$  we always have  $(L_k)^n|F\rangle = 0$ . A direct corollary of Eq. (B1) is

$$(L_k)^{2NS+1}|F\rangle \propto |-S, -S, \dots, -S\rangle. \quad (\text{B3})$$

To prove Eq. (B1), we first calculate  $[H, L_k]$  as

$$[H, L_k] = (J_z e^{ik} - J_{xy}) \sum_{n=1}^N e^{ikn} S_{n+1}^- S_n^z + (J_z - J_{xy} e^{ik}) \sum_{n=1}^N e^{ikn} S_n^- S_{n+1}^z. \quad (\text{B4})$$

By applying  $[H, L_k]$  to  $|F\rangle$ , we obtain

$$\begin{aligned} [H, L_k]|F\rangle &= S(J_z e^{ik} - J_{xy}) \sum_{n=1}^N e^{ikn} S_{n+1}^- |F\rangle + S(J_z - J_{xy} e^{ik}) \sum_{n=1}^N e^{ikn} S_n^- |F\rangle \\ &= 2S(J_z - J_{xy} \cos k)L_k|F\rangle \\ &= 0, \end{aligned} \quad (\text{B5})$$

which proves Eq. (B1) for  $n = 1$ . We now observe that the following commutator

$$[L_k, [H, L_k]] = -2e^{ik}(J_z - J_{xy} \cos k) \sum_n e^{i2kn} S_{n+1}^- S_n^- \quad (\text{B6})$$

vanishes under the condition given by (B2), so that

$$\begin{aligned} 0 &= [L_k, [H, L_k]]|F\rangle \\ &= L_k H L_k |F\rangle - L_k^2 H |F\rangle - H L_k^2 |F\rangle + L_k H L_k |F\rangle \\ &= -H L_k^2 |F\rangle + E_F L_k^2 |F\rangle, \end{aligned} \quad (\text{B7})$$

which proves Eq. (B1) for  $n = 2$ . Following Refs. [4, 5], we assume Eq. (B1) holds for  $l$  and  $l + 1$ , i.e.,  $H(L_k)^l |F\rangle = E_F(L_k)^l |F\rangle$  and  $H(L_k)^{l+1} |F\rangle = E_F(L_k)^{l+1} |F\rangle$ . Then,

$$\begin{aligned} 0 &= [L_k, [H, L_k]](L_k)^l |F\rangle \\ &= L_k H L_k (L_k)^l |F\rangle - L_k^2 H (L_k)^l |F\rangle - H L_k^2 (L_k)^l |F\rangle + L_k H L_k (L_k)^l |F\rangle \\ &= -H (L_k)^{l+2} |F\rangle + E_F L_k^{l+2} |F\rangle. \end{aligned} \quad (\text{B8})$$

By mathematical induction, we therefore proved Eq. (B1) for all  $n \leq 2NS + 1$ .

## 2. The zero-energy state $(L_k)^2 |F\rangle$ as a zero-energy Bloch state

The ZES  $(L_k)^2 |F\rangle$  under the condition  $J_z = J_{xy} \cos k$ ,  $k \in K_0$  must be a zero-energy state of certain Bloch Hamiltonian  $\mathcal{H}_2(p) - E_F$ , where the wave number  $p = p(k)$  depends on the value of  $k$ . To find out the relation between  $k$  and  $p$ , let us calculate  $(L_k)^2 |F\rangle$  explicitly:

$$\begin{aligned} L_k^2 |F\rangle &= \left( \sum_{n=1}^N e^{ikn} S_n^- \right) \left( \sum_{m=1}^N e^{ikm} S_m^- \right) |F\rangle \\ &= \sum_{n=1}^N e^{i2kn} (S_n^-)^2 |F\rangle + 2 \sum_{n < m} e^{ik(n+m)} S_n^- S_m^- |F\rangle \\ &= 2\sqrt{S(2S-1)} \sum_{n=1}^N e^{i2kn} T^{n-1} |1, 1\rangle + 4S \sum_{r=1}^{N/2-1} \sum_{n=1}^N e^{ik(2n+r)} T^{n-1} |1, 1+r\rangle \\ &\quad + 4S \sum_{n=1}^{N/2} e^{ik(2n+N/2)} T^{n-1} |1, 1+N/2\rangle. \end{aligned} \quad (\text{B9})$$

Using

$$\begin{aligned} T^n |1, 1+r\rangle &= \frac{1}{\sqrt{N}} \sum_{k \in K_0} e^{-ikn} e^{-i\frac{rk}{2}} |\psi_r(k)\rangle, \quad r = 0, 1, \dots, N/2 - 1, \\ T^n |1, 1 + \frac{N}{2}\rangle &= \sqrt{\frac{2}{N}} \sum_{k \in K_1} e^{-ikn} e^{-i\frac{Nk}{4}} |\psi_{N/2}(k)\rangle, \end{aligned} \quad (\text{B10})$$

we get

$$\begin{aligned} L_k^2 |F\rangle &= 2\sqrt{S(2S-1)} \frac{1}{\sqrt{N}} \sum_{k' \in K_0} \sum_{n=1}^N e^{i(2k-k')n} e^{ik'} |\psi_0(k')\rangle \\ &\quad + 4S \sum_{r=1}^{N/2-1} \frac{1}{\sqrt{N}} \sum_{k' \in K_0} \sum_{n=1}^N e^{i(2k-k')n} e^{\frac{i}{2}(2k-k')r} e^{ik'} |\psi_r(k')\rangle \\ &\quad + 4S \sqrt{\frac{2}{N}} \sum_{k' \in K_1} \sum_{n=1}^{N/2} e^{i(2k-k')n} e^{ik'} e^{\frac{i}{4}N(2k-k')} |\psi_{N/2}(k')\rangle. \end{aligned} \quad (\text{B11})$$



**Appendix C: Effective Hamiltonian analysis for  $D = 0$  and small  $J_{xy}/J_z$**

Consider a general Hamiltonian

$$h = h_0 + \lambda V, \quad (\text{C1})$$

in which  $\lambda V$  can be viewed as a perturbation. Let  $P_0$  denote the projector on the degenerate manifold associated with eigenvalue  $E_0$  of  $h_0$ , then the Takahashi effective Hamiltonian up to the third order of  $\lambda$  in this manifold reads [6]

$$h_{\text{eff}} = E_0 P_0 + \lambda P_0 V P_0 + \lambda^2 P_0 V S^1 V P_0 + \lambda^3 \left( P_0 V S^1 V S^1 V P_0 - \frac{1}{2} P_0 V S^2 V P_0 V P_0 - \frac{1}{2} P_0 V P_0 V S^2 V P_0 \right), \quad (\text{C2})$$

where  $S^k = \left( \frac{1 - P_0}{E_0 - h_0} \right)^k$ ,  $k \geq 1$ .

We now apply the above theory to the Bloch Hamiltonian  $\mathcal{H}_3(k) - E_F$  in the case of  $D = 0$ . The nonperturbative ground-state manifold is spanned by  $\{|\psi_{0,1}\rangle, |\psi_{0,N-1}\rangle, |\psi_{1,1}\rangle\}$  with common energy  $E_0 = (6S - 2)J_z$ , so that

$$P_0 = |\psi_{0,1}\rangle\langle\psi_{0,1}| + |\psi_{0,N-1}\rangle\langle\psi_{0,N-1}| + |\psi_{1,1}\rangle\langle\psi_{1,1}|. \quad (\text{C3})$$

After a straightforward calculation we obtain a  $3 \times 3$  effective Hamiltonian with the following matrix elements

$$\begin{aligned} [\mathcal{H}_{3,D=0}^{(\text{eff})}(k) - E_F]_{1,1} &= [\mathcal{H}_{3,D=0}^{(\text{eff})}(k) - E_F]_{2,2} = \frac{S(4S-3)J_{xy}^2(2S-1)J_{xy}\cos k - 2J_z}{4J_z J_z}, \\ [\mathcal{H}_{3,D=0}^{(\text{eff})}(k) - E_F]_{1,1} &= -\frac{S J_{xy}^2 2J_z(4S-1) + J_{xy}S(10S-3)\cos k}{2J_z J_z}, \\ [\mathcal{H}_{3,D=0}^{(\text{eff})}(k) - E_F]_{1,2} &= z^{-(N+1)} J_{xy} \left[ -(2S-1) - \frac{J_{xy}3S(S-1)z^3}{2J_z} + \frac{J_{xy}^2 S(2S-1)(5S-3)}{4J_z^2} \right], \\ [\mathcal{H}_{3,D=0}^{(\text{eff})}(k) - E_F]_{1,3} &= \sqrt{S(2S-1)} J_{xy} \left[ -z - \frac{J_{xy}S z^{-2}}{2J_z} + \frac{J_{xy}^2 z S(17S-9)}{8J_z^2} \right], \\ [\mathcal{H}_{3,D=0}^{(\text{eff})}(k) - E_F]_{2,3} &= z^N \sqrt{S(2S-1)} J_{xy} \left[ -z^{-1} - \frac{J_{xy}S z^2}{2J_z} + \frac{J_{xy}^2 S(17S-9)}{8J_z^2 z} \right]. \end{aligned} \quad (\text{C4})$$

**Appendix D: Fourth order energy correction for  $D/J_z > 1/2$  and  $\frac{J_{xy}}{2D-J_z} < 1$**

For  $D/J_z > 1/2$ , the ground state  $|\psi_{0,0}(k)\rangle$  is nondegenerate and has excitation energy  $\mathcal{E}^{(0)}(k) = 6SJ_z + D(6S-9)$ . The first order energy correction  $\mathcal{E}^{(1)}(k)$  vanishes. The second order correction is

$$\mathcal{E}^{(2)}(k) = \sum_a \frac{|V_{0,0;a}|^2}{\varepsilon_{0,0;a}} = J_{xy}^2 \frac{|t_g z|^2 + |t_g z^{N-1}|^2}{\varepsilon_{0,0} - \varepsilon_{0,1}} = \frac{J_{xy}^2 t_g^2}{J_z - 2D}. \quad (\text{D1})$$

We may also encounter

$$\epsilon^{(2)} = \sum_a \frac{|V_{0,0;a}|^2}{\varepsilon_{0,0;a}^2} = J_{xy}^2 \frac{|t_g z|^2 + |t_g z^{N-1}|^2}{(\varepsilon_{0,0} - \varepsilon_{0,1})^2} = \frac{J_{xy}^2 t_g^2}{2(J_z - 2D)^2}. \quad (\text{D2})$$

The third order correction is

$$\mathcal{E}^{(3)}(k) = \sum_{a_1, a_2} \frac{V_{0,0;a_2} V_{a_2 a_1} V_{a_1;0,0}}{\varepsilon_{0,0;a_1} \varepsilon_{0,0;a_2}}. \quad (\text{D3})$$

Note that  $a_1$  and  $a_2$  can be either  $(0, 1)$  or  $(0, N-1)$ , and  $a_1 \neq a_2$ . So only two terms with  $(a_1, a_2) = ((0, 0), (0, N-1))$  and  $(a_1, a_2) = ((0, N-1), (0, 0))$  contribute to the summation over  $a_1$  and  $a_2$ :

$$\begin{aligned} \mathcal{E}^{(3)}(k) &= \frac{V_{0,0;0,1} V_{0,1;0,N-1} V_{0,N-1;0,0}}{\varepsilon_{0,0;0,1}^2} + \text{c.c.} = (-J_{xy})^3 \frac{t_g z^{1-N} t_y z^{1+N} t_g z + \text{c.c.}}{4(J_z - 2D)^2} \\ &= (-J_{xy})^3 \frac{t_g^2 t_y (z^3 + \text{c.c.})}{4(J_z - 2D)^2} = (-J_{xy})^3 \frac{t_g^2 t_y \cos k}{2(J_z - 2D)^2}. \end{aligned} \quad (\text{D4})$$

The fourth order correction is

$$\mathcal{E}^{(4)}(k) = \sum_{a_1 a_2 a_3} \frac{V_{0,0;a_3} V_{a_3;a_2} V_{a_2;a_1} V_{a_1;0,0}}{\varepsilon_{0,0;a_1} \varepsilon_{0,0;a_2} \varepsilon_{0,0;a_3}} - \mathcal{E}^{(2)}(k) \varepsilon^{(2)}. \quad (\text{D5})$$

Note that  $(a_1, a_3)$  can only be  $((0, 1), (0, 1))$ ,  $((0, 1), (0, N-1))$ ,  $((0, N-1), (0, 1))$ , and  $((0, N-1), (0, N-1))$ , and  $a_2 \neq (0, 0)$  otherwise  $\varepsilon_{0,0;a_2} = 0$ . From

$$\begin{aligned} H_{XY}|\psi_{0,0}\rangle &= t_g z |\psi_{0,1}\rangle + t_g z^{N-1} |\psi_{0,N-1}\rangle, \\ H_{XY}|\psi_{0,1}\rangle &= t_g z^{-1} |\psi_{0,0}\rangle + t_y z^{N+1} |\psi_{0,N-1}\rangle + t_p z^{-1} |\psi_{1,1}\rangle + t_b z |\psi_{0,2}\rangle, \\ H_{XY}|\psi_{0,N-1}\rangle &= t_g z^{1-N} |\psi_{0,0}\rangle + t_y z^{-(N+1)} |\psi_{0,1}\rangle + t_p z^{1-N} |\psi_{1,1}\rangle + t_b z^{-1} |\psi_{0,N-2}\rangle \end{aligned}$$

we have

$$\begin{aligned} & \sum_{a_1 a_2 a_3} \frac{V_{0,0;a_3} V_{a_3;a_2} V_{a_2;a_1} V_{a_1;0,0}}{\varepsilon_{0,0;a_1} \varepsilon_{0,0;a_2} \varepsilon_{0,0;a_3}} \\ &= \sum_{a_2} \frac{V_{0,0;0,1} V_{0,1;a_2} V_{a_2;0,1} V_{0,1;0,0}}{\varepsilon_{0,0;0,1} \varepsilon_{0,0;a_2} \varepsilon_{0,0;0,1}} + \sum_{a_2} \frac{V_{0,0;0,N-1} V_{0,N-1;a_2} V_{a_2;0,1} V_{0,1;0,0}}{\varepsilon_{0,0;0,1} \varepsilon_{0,0;a_2} \varepsilon_{0,0;0,1}} \\ &+ \sum_{a_2} \frac{V_{0,0;0,1} V_{0,1;a_2} V_{a_2;0,N-1} V_{0,N-1;0,0}}{\varepsilon_{0,0;0,1} \varepsilon_{0,0;a_2} \varepsilon_{0,0;0,1}} + \sum_{a_2} \frac{V_{0,0;0,N-1} V_{0,N-1;a_2} V_{a_2;0,N-1} V_{0,N-1;0,0}}{\varepsilon_{0,0;0,1} \varepsilon_{0,0;a_2} \varepsilon_{0,0;0,1}} \\ &= \frac{|V_{0,1;0,0}|^2}{\varepsilon_{0,0;0,1}^2} \left( \frac{|V_{0,2;0,1}|^2}{\varepsilon_{0,0} - \varepsilon_{0,2}} + \frac{|V_{0,N-1;0,1}|^2}{\varepsilon_{0,0} - \varepsilon_{0,N-1}} + \frac{|V_{1,1;0,1}|^2}{\varepsilon_{0,0} - \varepsilon_{1,1}} \right) + \left( \frac{V_{0,0;0,N-1} V_{0,1;0,0}}{\varepsilon_{0,0;0,1}^2} \frac{V_{0,N-1;1,1} V_{1,1;0,1}}{\varepsilon_{0,0;1,1}} + c.c. \right) \\ &+ \frac{|V_{0,N-1;0,0}|^2}{\varepsilon_{0,0;0,1}^2} \left( \frac{|V_{0,1;0,N-1}|^2}{\varepsilon_{0,0;0,1}} + \frac{|V_{0,N-2;0,N-1}|^2}{\varepsilon_{0,0;0,N-2}} + \frac{|V_{1,1;0,N-1}|^2}{\varepsilon_{0,0;1,1}} \right) \\ &= J_{xy}^4 \frac{t_g^2}{4(J_z - 2D)^2} \left( \frac{t_b^2}{-2D} + \frac{t_y^2}{J_z - 2D} + \frac{2t_p^2}{J_z - 3D} \right). \quad (\text{D6}) \end{aligned}$$

So

$$\mathcal{E}^{(4)}(k) = J_{xy}^4 \frac{3S(S-1)}{4(J_z - 2D)^2} \left[ \frac{2S(2S-1)}{J_z - 3D} - \frac{S^2}{2D} - \frac{2S^2 - 2S - 1}{J_z - 2D} \right]. \quad (\text{D7})$$

which only induces a constant energy shift.

### Appendix E: Time-dependent perturbation for $S \geq \frac{3}{2}$ , $D/J_z > \frac{1}{2}$ , $|\Phi(0)\rangle = |\phi_{0,0}^{\frac{N}{2}-1}\rangle = |\frac{N}{2}, \frac{N}{2}, \frac{N}{2}\rangle$

We first write the initial state  $|\Phi(0)\rangle = |\frac{N}{2}, \frac{N}{2}, \frac{N}{2}\rangle$  in terms of the Bloch basis states as

$$|\Phi(0)\rangle = |\frac{N}{2}, \frac{N}{2}, \frac{N}{2}\rangle = \frac{1}{\sqrt{N}} \sum_{k \in K_0} e^{-ik(N/2-1)} |\psi_{0,0}(k)\rangle. \quad (\text{E1})$$

We next expand the time-evolution operator to the second order of  $-J_{xy} H_{XY}$  as

$$e^{-iHt} \approx e^{-iH_0 t} (1 + U_1 + U_2), \quad (\text{E2})$$

where

$$\begin{aligned} U_1 &= iJ_{xy} \int_0^t ds H_{XY}(s), \\ U_2 &= -J_{xy}^2 \int_0^t ds \int_0^s ds' H_{XY}(s) H_{XY}(s'), \end{aligned} \quad (\text{E3})$$

with  $H_{XY}(s) = e^{iH_0 s} H_{XY} e^{-iH_0 s}$ . The expectation value of an observable  $O$  at time  $t$  can be approximated as

$$\begin{aligned} O(t) &\approx \langle \Phi(0) | (1 + U_1^\dagger + U_2^\dagger) e^{iH_0 t} O e^{-iH_0 t} (1 + U_1 + U_2) | \Phi(0) \rangle \\ &= O^{(0)}(t) + O^{(1)}(t) + O^{(2)}(t), \end{aligned} \quad (\text{E4})$$

where

$$O^{(0)}(t) = \langle \Phi(0) | e^{iH_0 t} O e^{-iH_0 t} | \Phi(0) \rangle, \quad (E5)$$

$$O^{(1)}(t) = \langle \Phi(0) | e^{iH_0 t} O e^{-iH_0 t} U_1 | \Phi(0) \rangle + \text{c.c.} \quad (E6)$$

and

$$O^{(2)}(t) = [\langle \Phi(0) | e^{iH_0 t} O e^{-iH_0 t} U_2 | \Phi(0) \rangle + \text{c.c.}] + \langle \Phi(0) | U_1^\dagger e^{iH_0 t} O e^{-iH_0 t} U_1 | \Phi(0) \rangle, \quad (E7)$$

are the zeroth-order, first-order, and second-order contributions, respectively.

We are interested in the dynamics of the local magnetization  $S_j^z$ . By noting that  $\langle \psi_{r_1 r_2}(k') | S_j^z | \psi_{r_1 r_2}(k) \rangle \propto \delta_{r_1 r_1'} \delta_{r_2 r_2'}$ , we have

1) Zeroth order:

$$\begin{aligned} \langle S_j^{z,(0)}(t) \rangle &= \langle \Phi(0) | e^{iH_0 t} S_j^z e^{-iH_0 t} | \Phi(0) \rangle \\ &= \frac{1}{\sqrt{N}} \sum_{k'} e^{ik'(N/2-1)} \langle \psi_{0,0}(k') | e^{iH_0 t} S_j^z e^{-iH_0 t} \frac{1}{\sqrt{N}} \sum_k e^{-ik(N/2-1)} | \psi_{0,0}(k) \rangle \\ &= \frac{1}{N} \sum_{kk'} e^{i(k'-k)(N/2-1)} e^{i\varepsilon_{0,0} t} e^{-i\varepsilon_{0,0} t} \langle \psi_{0,0}(k') | S_j^z | \psi_{0,0}(k) \rangle \\ &= \frac{1}{N} \sum_{kk'} e^{i(k'-k)(N/2-1)} \langle \psi_{0,0}(k') | S_j^z | \psi_{0,0}(k) \rangle \\ &= \langle \frac{N}{2}, \frac{N}{2}, \frac{N}{2} | S_j^z | \frac{N}{2}, \frac{N}{2}, \frac{N}{2} \rangle, \end{aligned} \quad (E8)$$

which is just the initial value of  $S_j^z$  in the initial state  $|\frac{N}{2}, \frac{N}{2}, \frac{N}{2}\rangle$ .

2) First order:

$$\begin{aligned} \langle S_j^{z,(1)}(t) \rangle &= \langle \Phi(0) | e^{iH_0 t} S_j^z e^{-iH_0 t} U_1 | \Phi(0) \rangle + \text{c.c.} \\ &= \frac{1}{\sqrt{N}} \sum_{k'} e^{ik'(N/2-1)} \langle \psi_{0,0}(k') | e^{iH_0 t} S_j^z e^{-iH_0 t} iJ_{xy} \int_0^t ds H_{XY}(s) \frac{1}{\sqrt{N}} \sum_k e^{-ik(N/2-1)} | \psi_{0,0}(k) \rangle + \text{c.c.} \\ &= 0, \end{aligned} \quad (E9)$$

which indeed vanishes.

2) Second order:

The first part is

$$\begin{aligned} \langle S_{j,1}^{z,(2)}(t) \rangle &= [\langle \Phi(0) | e^{iH_0 t} S_j^z e^{-iH_0 t} U_2 | \Phi(0) \rangle + \text{c.c.}] \\ &= -\frac{J_{xy}^2}{\sqrt{N}} \sum_{k'} e^{ik'(N/2-1)} \langle \psi_{0,0}(k') | e^{iH_0 t} S_j^z e^{-iH_0 t} \int_0^t ds \int_0^s ds' H_{XY}(s) H_{XY}(s') \frac{1}{\sqrt{N}} \sum_k e^{-ik(N/2-1)} | \psi_{0,0}(k) \rangle + \text{c.c.} \\ &= -\frac{J_{xy}^2}{N} \sum_{k'} \sum_k e^{i(k'-k)(N/2-1)} \langle \psi_{0,0}(k') | e^{iH_0 t} S_j^z e^{-iH_0 t} \int_0^t ds \int_0^s ds' H_{XY}(s) H_{XY}(s') | \psi_{0,0}(k) \rangle + \text{c.c.} \\ &= -2 \frac{J_{xy}^2}{N} \sum_{k'} \sum_k e^{i(k'-k)(N/2-1)} \langle \psi_{0,0}(k') | e^{iH_0 t} S_j^z e^{-iH_0 t} t_g^2 \frac{1 + it\varepsilon_{pb} - e^{i\varepsilon_{pb}t}}{\varepsilon_{pb}^2} | \psi_{0,0}(k) \rangle + \text{c.c.} \\ &= -2 \frac{J_{xy}^2}{N} \sum_{k'} \sum_k e^{i(k'-k)(N/2-1)} \langle \psi_{0,0}(k') | S_j^z | \psi_{0,0}(k) \rangle t_g^2 \frac{1 + it\varepsilon_{pb} - e^{i\varepsilon_{pb}t}}{\varepsilon_{pb}^2} + \text{c.c.} \\ &= -2 J_{xy}^2 \langle \frac{N}{2}, \frac{N}{2}, \frac{N}{2} | S_j^z | \frac{N}{2}, \frac{N}{2}, \frac{N}{2} \rangle t_g^2 \frac{1 + it\varepsilon_{pb} - e^{i\varepsilon_{pb}t}}{\varepsilon_{pb}^2} + \text{c.c.} \\ &= -2 J_{xy}^2 \langle \frac{N}{2}, \frac{N}{2}, \frac{N}{2} | S_j^z | \frac{N}{2}, \frac{N}{2}, \frac{N}{2} \rangle t_g^2 \frac{1 + it\varepsilon_{pb} - e^{i\varepsilon_{pb}t} + 1 - it\varepsilon_{pb} - e^{-i\varepsilon_{pb}t}}{\varepsilon_{pb}^2} \\ &= -4 J_{xy}^2 \langle \frac{N}{2}, \frac{N}{2}, \frac{N}{2} | S_j^z | \frac{N}{2}, \frac{N}{2}, \frac{N}{2} \rangle t_g^2 \frac{1 - \cos \varepsilon_{pb}t}{\varepsilon_{pb}^2}, \end{aligned} \quad (E10)$$

where

$$\varepsilon_{pb} = \varepsilon_p - \varepsilon_b = 2(J_z - 2D), \quad (\text{E11})$$

is the energy difference between the  $p$ -state and the  $b$ -states.

The second part can be similarly calculated as

$$S_{j,2}^{z,(2)}(t) = 2J_{xy}^2 t_g^2 \frac{1 - \cos \varepsilon_{pb} t}{\varepsilon_{pb}^2} \left[ \langle \frac{N}{2}, \frac{N}{2}, \frac{N}{2} + 1 | S_j^z | \frac{N}{2}, \frac{N}{2}, \frac{N}{2} + 1 \rangle + \langle \frac{N}{2}, \frac{N}{2}, \frac{N}{2} - 1 | S_j^z | \frac{N}{2}, \frac{N}{2}, \frac{N}{2} - 1 \rangle \right]. \quad (\text{E12})$$

Note that

$$\begin{aligned} \langle \frac{N}{2}, \frac{N}{2}, \frac{N}{2} | S_j^z | \frac{N}{2}, \frac{N}{2}, \frac{N}{2} \rangle &= S - 3\delta_{j, \frac{N}{2}}, \\ \langle \frac{N}{2}, \frac{N}{2}, \frac{N}{2} + 1 | S_j^z | \frac{N}{2}, \frac{N}{2}, \frac{N}{2} + 1 \rangle &= S - 2\delta_{j, \frac{N}{2}} - \delta_{j, \frac{N}{2}+1}, \\ \langle \frac{N}{2}, \frac{N}{2}, \frac{N}{2} - 1 | S_j^z | \frac{N}{2}, \frac{N}{2}, \frac{N}{2} - 1 \rangle &= S - 2\delta_{j, \frac{N}{2}} - \delta_{j, \frac{N}{2}-1}, \end{aligned} \quad (\text{E13})$$

we finally get

$$S_j^z(t) \approx S - 3\delta_{j, \frac{N}{2}} + 2J_{xy}^2 t_g^2 \frac{1 - \cos \varepsilon_{pb} t}{\varepsilon_{pb}^2} (2\delta_{j, \frac{N}{2}} - \delta_{j, \frac{N}{2}+1} - \delta_{j, \frac{N}{2}-1}). \quad (\text{E14})$$

## Appendix F: Magnon dynamics based on magnon bound state analysis

Suppose the initial state is a localized state:

$$|\Phi(0)\rangle = |\phi_{r_1, r_2}^n\rangle = T^n |1, 1 + r_1, 1 + r_1 + r_2\rangle = \frac{1}{\sqrt{N}} \sum_{k \in K_0} |\Phi_k(0)\rangle, \quad (\text{F1})$$

where

$$|\Phi_k(0)\rangle = e^{-ikn} e^{-i\frac{k}{3}(2r_1+r_2)} |\psi_{r_1, r_2}(k)\rangle. \quad (\text{F2})$$

is the initial component state in the  $k$ -subspace. The eigenstates  $\{|\Psi_\alpha(k)\rangle\}$  and the Bloch state  $\{|\psi_a(k)\rangle\}$  in the  $k$ -subspace both satisfy the completeness relation

$$\sum_{\alpha} |\Psi_\alpha(k)\rangle \langle \Psi_\alpha(k)| = \sum_a |\psi_a(k)\rangle \langle \psi_a(k)| = 1_k, \quad (\text{F3})$$

which gives

$$|\Phi_k(0)\rangle = e^{-ikn} e^{-i\frac{k}{3}(2r_1+r_2)} \sum_{\alpha} \langle \Psi_\alpha(k) | \psi_{r_1, r_2}(k) \rangle |\Psi_\alpha(k)\rangle. \quad (\text{F4})$$

The time-evolved state is thus

$$\begin{aligned} |\Phi_k(t)\rangle &= e^{-iH_3(k)t} |\Phi_k(0)\rangle \\ &= e^{-ikn} e^{-i\frac{k}{3}(2r_1+r_2)} \sum_{\alpha} \langle \Psi_\alpha(k) | \psi_{r_1, r_2}(k) \rangle e^{-iE_\alpha(k)t} |\Psi_\alpha(k)\rangle \\ &= e^{-ikn} e^{-i\frac{k}{3}(2r_1+r_2)} \sum_{\alpha} \sum_{s_1 s_2}^{(m-1, m+1)} \langle \Psi_\alpha(k) | \psi_{r_1, r_2}(k) \rangle e^{-iE_\alpha(k)t} \langle \psi_{s_1 s_2}(k) | \Psi_\alpha(k) \rangle \\ &\quad e^{(2s_1+s_2)i\frac{k}{3}} \frac{1}{\sqrt{N}} \sum_{l=0}^{N-1} e^{ikl} T^l |1, 1 + s_1, 1 + s_1 + s_2\rangle \\ &\quad + \delta_{k \in K_2} e^{-ikn} e^{-i\frac{k}{3}(2r_1+r_2)} \sum_{\alpha} \langle \Psi_\alpha(k) | \psi_{r_1, r_2}(k) \rangle e^{-iE_\alpha(k)t} \langle \psi_{m, m}(k) | \Psi_\alpha(k) \rangle \\ &\quad \frac{e^{ikm}}{\sqrt{m}} \sum_{l=0}^{m-1} e^{ikl} T^l |1, 1 + m, 1 + 2m\rangle. \end{aligned} \quad (\text{F5})$$

So

$$\begin{aligned}
|\Phi(t)\rangle &= \frac{1}{\sqrt{N}} \sum_k |\Phi_k(t)\rangle \\
&= \frac{1}{N} \sum_{l=0}^{N-1} \sum_k \sum_{s_1 s_2}^{(m-1, m+1)} e^{ik(l-n)} e^{i\frac{k}{3}[2(s_1-r_1)+(s_2-r_2)]} \sum_{\alpha} \langle \Psi_{\alpha}(k) | \psi_{r_1, r_2}(k) \rangle e^{-iE_{\alpha}(k)t} \langle \psi_{s_1 s_2}(k) | \Psi_{\alpha}(k) \rangle \\
&\quad T^l |1, 1 + s_1, 1 + s_1 + s_2\rangle \\
&\quad + \frac{1}{\sqrt{Nm}} \sum_{l=0}^{m-1} \sum_{k \in K_2} e^{ik(l-n)} e^{i\frac{k}{3}(3m-2r_1-r_2)} \sum_{\alpha} \langle \Psi_{\alpha}(k) | \psi_{r_1, r_2}(k) \rangle e^{-iE_{\alpha}(k)t} \langle \psi_{m, m}(k) | \Psi_{\alpha}(k) \rangle \\
&\quad T^l |1, 1 + m, 1 + 2m\rangle.
\end{aligned} \tag{F6}$$

We now define the quantity

$$F_{r_1 r_2; s_1 s_2}(k, t) \equiv \sum_{\alpha} \langle \Psi_{\alpha}(k) | \psi_{r_1, r_2}(k) \rangle e^{-iE_{\alpha}(k)t} \langle \psi_{s_1 s_2}(k) | \Psi_{\alpha}(k) \rangle, \tag{F7}$$

with initial condition

$$F_{r_1 r_2; s_1 s_2}(k, t=0) \equiv \delta_{r_1 s_1} \delta_{r_2 s_2}, \tag{F8}$$

then

$$\begin{aligned}
|\Phi(t)\rangle &= \frac{1}{N} \sum_{l=0}^{N-1} \sum_k \sum_{s_1 s_2}^{(m-1, m+1)} e^{ik(l-n)} e^{i\frac{k}{3}[2(s_1-r_1)+(s_2-r_2)]} F_{r_1 r_2; s_1 s_2}(k, t) T^l |1, 1 + s_1, 1 + s_1 + s_2\rangle \\
&\quad + \frac{1}{\sqrt{Nm}} \sum_{l=0}^{m-1} \sum_{k \in K_2} e^{ik(l-n)} e^{i\frac{k}{3}(3m-2r_1-r_2)} F_{r_1 r_2; m, m}(k, t) T^l |1, 1 + m, 1 + 2m\rangle.
\end{aligned} \tag{F9}$$

Using

$$\begin{aligned}
\langle 1, 1 + s_1, 1 + s_1 + s_2 | T^{-l} S_j^z T^l | 1, 1 + s_1, 1 + s_1 + s_2 \rangle &= S - \tilde{\delta}_{j-l, 1} - \tilde{\delta}_{j-l, 1+s_1} - \tilde{\delta}_{j-l, 1+s_1+s_2}, \\
\langle 1, 1 + m, 1 + 2m | T^{-l} S_j^z T^l | 1, 1 + m, 1 + 2m \rangle &= S - \delta_{j-l, 1} - \delta_{j-l, m+1} - \delta_{j-l, 2m+1},
\end{aligned} \tag{F10}$$

where  $\tilde{\delta}_{ij}$  is 1 when  $i = j + qN$  ( $q \in Z$ ) and 0 otherwise, we have

$$\begin{aligned}
\langle \Phi(t) | S_j^z | \Phi(t) \rangle &= \frac{1}{N^2} \sum_{kk'} \sum_{l=0}^{N-1} \sum_{s_1 s_2}^{(m-1, m+1)} e^{i(k-k')(l-n)} e^{i\frac{k-k'}{3}[2(s_1-r_1)+(s_2-r_2)]} F_{r_1 r_2; s_1 s_2}(k, t) F_{r_1 r_2; s_1 s_2}^*(k', t) \\
&\quad \langle 1, 1 + s_1, 1 + s_1 + s_2 | T^{-l} S_j^z T^l | 1, 1 + s_1, 1 + s_1 + s_2 \rangle \\
&\quad + \frac{1}{Nm} \sum_{kk' \in K_2} \sum_{l=0}^{m-1} e^{i(k-k')(l-n)} e^{i\frac{k-k'}{3}(3m-2r_1-r_2)} F_{r_1 r_2; m, m}(k, t) F_{r_1 r_2; m, m}^*(k', t) \\
&\quad \langle 1, 1 + m, 1 + 2m | T^{-l} S_j^z T^l | 1, 1 + m, 1 + 2m \rangle \\
&= \frac{S}{N} \sum_k \sum_{s_1 s_2}^{(m-1, m+1)} F_{r_1 r_2; s_1 s_2}(k, t) F_{r_1 r_2; s_1 s_2}^*(k, t) \\
&\quad - \frac{1}{N^2} \sum_{kk'} \sum_{s_1 s_2}^{(m-1, m+1)} e^{i(k-k')(j-1-n)} [1 + e^{-i(k-k')s_1} + e^{-i(k-k')(s_1+s_2)}] \\
&\quad e^{i\frac{k-k'}{3}[2(s_1-r_1)+(s_2-r_2)]} F_{r_1 r_2; s_1 s_2}(k, t) F_{r_1 r_2; s_1 s_2}^*(k', t) \\
&\quad + \frac{S}{N} \sum_{k \in K_2} F_{r_1 r_2; m, m}(k, t) F_{r_1 r_2; m, m}^*(k, t) \\
&\quad - \frac{1}{Nm} \sum_{kk' \in K_2} e^{i(k-k')(j-1-n)} e^{i\frac{k-k'}{3}(3m-2r_1-r_2)} F_{r_1 r_2; m, m}(k, t) F_{r_1 r_2; m, m}^*(k', t).
\end{aligned} \tag{F11}$$

We need to calculate the following quantities:

1)

$$\begin{aligned}
G_{r_1 r_2}(t) &\equiv \frac{S}{N} \left[ \sum_k \sum_{s_1 s_2}^{(m-1, m+1)} F_{r_1 r_2; s_1 s_2}(k, t) F_{r_1 r_2; s_1 s_2}^*(k, t) + \frac{S}{N} \sum_{k \in K_2} F_{r_1 r_2; m, m}(k, t) F_{r_1 r_2; m, m}^*(k, t) \right] \\
&= \frac{S}{N} \sum_{k \in K_2} \sum_{s_1 s_2}^{(m, m)} F_{r_1 r_2; s_1 s_2}(k, t) F_{r_1 r_2; s_1 s_2}^*(k, t) + \frac{S}{N} \sum_{k \in K'_2} \sum_{s_1 s_2}^{(m-1, m+1)} F_{r_1 r_2; s_1 s_2}(k, t) F_{r_1 r_2; s_1 s_2}^*(k, t). \quad (\text{F12})
\end{aligned}$$

Note that  $G_{r_1 r_2}(t)$  does not depend on  $j$  and  $n$  and can be viewed as a ‘background’ in the polarization dynamics. Actually,

$$\begin{aligned}
&\sum_{k \in K_2} \sum_{s_1 s_2}^{(m, m)} F_{r_1 r_2; s_1 s_2}(k, t) F_{r_1 r_2; s_1 s_2}^*(k, t) \\
&= \sum_{k \in K_2} \sum_{s_1 s_2}^{(m, m)} \sum_{\alpha} \langle \Psi_{\alpha}(k) | \psi_{r_1, r_2}(k) \rangle e^{-iE_{\alpha}(k)t} \langle \psi_{s_1 s_2}(k) | \Psi_{\alpha}(k) \rangle \sum_{\alpha'} \langle \psi_{r_1, r_2}(k) | \Psi_{\alpha'}(k) \rangle e^{iE_{\alpha'}(k)t} \langle \Psi_{\alpha'}(k) | \psi_{s_1 s_2}(k) \rangle \\
&= \sum_{k \in K_2} \sum_{\alpha} \sum_{\alpha'} \langle \Psi_{\alpha}(k) | \psi_{r_1, r_2}(k) \rangle e^{-iE_{\alpha}(k)t} \langle \psi_{r_1, r_2}(k) | \Psi_{\alpha'}(k) \rangle e^{iE_{\alpha'}(k)t} \delta_{\alpha \alpha'} \\
&= \sum_{k \in K_2} \sum_{\alpha} \langle \Psi_{\alpha}(k) | \psi_{r_1, r_2}(k) \rangle e^{-iE_{\alpha}(k)t} \langle \psi_{r_1, r_2}(k) | \Psi_{\alpha}(k) \rangle e^{iE_{\alpha}(k)t} \\
&= \sum_{k \in K_2} 1 \\
&= m. \quad (\text{F13})
\end{aligned}$$

Similarly, we have

$$\frac{S}{N} \sum_{k \in K'_2} \sum_{s_1 s_2}^{(m-1, m+1)} F_{r_1 r_2; s_1 s_2}(k, t) F_{r_1 r_2; s_1 s_2}^*(k, t) = 2m. \quad (\text{F14})$$

So

$$G_{r_1 r_2}(t) \equiv S, \quad (\text{F15})$$

which is actually independent of time  $t$ .

2)

$$\begin{aligned}
X_{r_1 r_2; s_1 s_2}^{(1), j, n}(t) &\equiv \frac{1}{N} \sum_k e^{ik(j-n-1)} e^{i\frac{k}{3}[2(s_1-r_1)+(s_2-r_2)]} F_{r_1 r_2; s_1 s_2}(k, t), \\
X_{r_1 r_2; s_1 s_2}^{(2), j, n}(t) &\equiv \frac{1}{N} \sum_k e^{ik(j-n-1-s_1)} e^{i\frac{k}{3}[2(s_1-r_1)+(s_2-r_2)]} F_{r_1 r_2; s_1 s_2}(k, t), \\
X_{r_1 r_2; s_1 s_2}^{(3), j, n}(t) &\equiv \frac{1}{N} \sum_k e^{ik[j-n-1-(s_1+s_2)]} e^{i\frac{k}{3}[2(s_1-r_1)+(s_2-r_2)]} F_{r_1 r_2; s_1 s_2}(k, t), \quad (\text{F16})
\end{aligned}$$

3)

$$Y_{r_1 r_2}^{j, n}(t) \equiv \frac{1}{\sqrt{Nm}} \sum_{k \in K_2} e^{ik(j-n-1)} e^{i\frac{k}{3}(3m-2r_1-r_2)} F_{r_1 r_2; mm}(k, t). \quad (\text{F17})$$

Using these quantities, we finally obtain

$$\langle \Phi(t) | S_j^z | \Phi(t) \rangle = S - \sum_{s_1 s_2}^{(m-1, m+1)} |X_{r_1 r_2; s_1 s_2}^{(1), j, n}(t)|^2 + |X_{r_1 r_2; s_1 s_2}^{(2), j, n}(t)|^2 + |X_{r_1 r_2; s_1 s_2}^{(3), j, n}(t)|^2 - |Y_{r_1 r_2}^{j, n}(t)|^2. \quad (\text{F18})$$

### Appendix G: Single-site reduced density matrix for $S = 1$

For  $S = 1$ , the most general form the reduced density matrix for spin  $j$  reads

$$\rho_j = \begin{pmatrix} 1 + \frac{1}{2}(a_j^z - q_j^{xx} - q_j^{yy}) & \frac{1}{2\sqrt{2}}[a_j^x + q_j^{zx} - i(a_j^y + q_j^{yz})] & \frac{1}{2}(q_j^{xx} - q_j^{yy} - iq_j^{xy}) \\ \frac{1}{2\sqrt{2}}[a_j^x + q_j^{zx} + i(a_j^y + q_j^{yz})] & -1 + q_j^{xx} + q_j^{yy} & \frac{1}{2\sqrt{2}}[a_j^x - q_j^{zx} - i(a_j^y - q_j^{yz})] \\ \frac{1}{2}(q_j^{xx} - q_j^{yy} + iq_j^{xy}) & \frac{1}{2\sqrt{2}}[a_j^x - q_j^{zx} + i(a_j^y - q_j^{yz})] & 1 - \frac{1}{2}(a_j^z + q_j^{xx} + q_j^{yy}) \end{pmatrix}, \quad (\text{G1})$$

where

$$\begin{aligned} a_j^\alpha &= \langle S_j^\alpha \rangle, \quad \alpha = x, y, z, \\ q_j^{\alpha\alpha} &= \langle (S_j^\alpha)^2 \rangle, \quad \alpha = x, y, \\ q_j^{\alpha\beta} &= \langle S_j^\alpha S_j^\beta + S_j^\beta S_j^\alpha \rangle, \quad \alpha\beta = xy, yz, zx. \end{aligned} \quad (\text{G2})$$

Since the total magnetization is conserved, if we start with an initial state with fixed  $M$ , then the evolved state  $|\psi(t)\rangle$  also belongs to the  $M$ -sector. We thus have

$$\begin{aligned} a_j^x &= a_j^y = 0, \quad a_j^z = \langle S_j^z \rangle, \\ q_j^{xx} &= q_j^{yy} = \frac{1}{4}\langle S_j^+ S_j^- + S_j^- S_j^+ \rangle, \quad \alpha = x, y, \\ q_j^{xy} &= q_j^{yz} = q_j^{zx} = 0. \end{aligned} \quad (\text{G3})$$

Thus,  $\rho_j$  reduces to

$$\rho_j = \begin{pmatrix} 1 + \frac{1}{2}\langle S_j^z \rangle - \frac{1}{4}\langle S_j^+ S_j^- + S_j^- S_j^+ \rangle & 0 & 0 \\ 0 & -1 + \frac{1}{2}\langle S_j^+ S_j^- + S_j^- S_j^+ \rangle & 0 \\ 0 & 0 & 1 - \frac{1}{2}\langle S_j^z \rangle - \frac{1}{4}\langle S_j^+ S_j^- + S_j^- S_j^+ \rangle \end{pmatrix} \quad (\text{G4})$$

In the standard basis with  $S_j^z = \begin{pmatrix} 1 & 0 & 0 \\ 0 & 0 & 0 \\ 0 & 0 & -1 \end{pmatrix}$ , we have  $S_j^+ = \sqrt{2} \begin{pmatrix} 0 & 1 & 0 \\ 0 & 0 & 1 \\ 0 & 0 & 0 \end{pmatrix}$  and  $S_j^- = \sqrt{2} \begin{pmatrix} 0 & 0 & 0 \\ 1 & 0 & 0 \\ 0 & 1 & 0 \end{pmatrix}$ , so that

$$S_j^+ S_j^- + S_j^- S_j^+ = 2 \begin{pmatrix} 1 & 0 & 0 \\ 0 & 2 & 0 \\ 0 & 0 & 1 \end{pmatrix}. \quad (\text{G5})$$

For arbitrary  $S$ , we get from  $\frac{1}{2}(S_j^+ S_j^- + S_j^- S_j^+) + (S_j^z)^2 = S(S+1)$

$$\frac{1}{2}\langle S_j^+ S_j^- + S_j^- S_j^+ \rangle = S(S+1) - \langle (S_j^z)^2 \rangle. \quad (\text{G6})$$

Thus, for  $S = 1$  we have

$$\rho_j = \begin{pmatrix} \frac{1}{2}[\langle (S_j^z)^2 \rangle + \langle S_j^z \rangle] & 0 & 0 \\ 0 & 1 - \langle (S_j^z)^2 \rangle & 0 \\ 0 & 0 & \frac{1}{2}[\langle (S_j^z)^2 \rangle - \langle S_j^z \rangle] \end{pmatrix}. \quad (\text{G7})$$

which is diagonal and only depends on  $\langle S_j^z \rangle$  and  $\langle (S_j^z)^2 \rangle$ .

### Appendix H: Maximization of $\bar{S}^{(\sigma)}(t) = -\sum_{n=0,\pm 1} P_n \ln P_n$

To maximize  $\bar{S}^{(\sigma)}(t) = -\sum_{n=0,\pm 1} P_n \ln P_n$  under the constraints of probability normalization  $\sum_{i=0,\pm 1} P_i = 1$  and magnetization conservation  $\sum_{i=0,\pm 1} iP_i = (N-3)/N$ , we introduce two Lagrangian multipliers  $\lambda_1$  and  $\lambda_2$  to write

$$\bar{S}^{(\sigma)}(t) = -\sum_{n=0,\pm 1} P_n \ln P_n + \lambda_1 \left( \sum_{n=0,\pm 1} P_n - 1 \right) + \lambda_2 \left[ \sum_{n=0,\pm 1} nP_n - (N-3)/N \right]. \quad (\text{H1})$$

By requiring that  $\delta\bar{S}^{(\sigma)}(t) = 0$ , we obtain

$$\sum_{n=0,\pm 1} \delta P_n (\ln P_n + 1 - \lambda_1 - n\lambda_2) = 0, \quad (\text{H2})$$

which is possible only if

$$P_n = e^{\lambda_1 - 1 + n\lambda_2}. \quad (\text{H3})$$

Combining with the two constraints, we get

$$P_1 = \frac{1}{Z} \frac{N - 3 + \sqrt{N^2 + 18N - 27}}{6}, \quad P_0 = \frac{1}{Z}, \quad P_{-1} = \frac{1}{Z} \frac{6}{N - 3 + \sqrt{N^2 + 18N - 27}}, \quad (\text{H4})$$

where  $Z = \frac{N - 3 + \sqrt{N^2 + 18N - 27}}{6} + \frac{6}{N - 3 + \sqrt{N^2 + 18N - 27}} + 1$ .

- 
- [1] R. Silbergliitt and J. B. Torrance, Jr., Phys. Rev. B **2**, 772 (1970).
  - [2] N. Papanicolaou and G. C. Psaltakis, Phys. Rev. B **35**, 342 (1987).
  - [3] Following Ref. [2], we still use the terminology “single-ion” and “exchange” for a state within the Brillouin zone if it is dominated by the corresponding bare component.
  - [4] C. D. Batista, Phys. Rev. B **80**, 180406(R) (2009).
  - [5] J. Wouters, H. Katsura, and D. Schuricht, Phys. Rev. B **98**, 155119 (2018).
  - [6] M. Takahashi, J. Phys. C **10**, 1289 (1977).